EARTHQUAKE MOTIONS AT AN EMBANKMENT DAM BASE AND AN ESTIMATION METHOD OF INCIDENT SEISMIC WAVES USING THE OBSERVATIONS

Yoshikazu Yamaguchi[1] & Tomoya Iwashita[2]

ABSTRACT

Many earthquake motions have been observed at the bedrock of embankment dams. The observed waves are affected by the dynamic interaction between the dam and its foundation. The effects of the frequency contents of the input waves and the impedance ratio on the dynamic interaction at the dam base were evaluated using FEM analyses. The change of the dynamic interaction on the footprint of dams was represented analytically. The analytical results agreed with the earthquake observations and the microtremor measurements at the dam sites. Moreover, a simplified analytical procedure to estimate incident seismic wave on the basement layer from the within motion observed at the base of an embankment dam was proposed. The procedure was applied to the estimation of the incident wave at a rockfill dam site during the Kobe Earthquake.

KEYWORDS: Dam, FEM, Earthquake Record, Dynamic Interaction, Incident Wave

1. INTRODUCTION

Earthquake observations at the bedrock of dam sites are precious data of earthquake motions at the hard rock site condition, for which the S-wave velocity is over about 800 m/s. There are few earthquake observational stations situated at hard rock sites in Japan, other than dams and nuclear power plants. In most dams in Japan, in particular, seismographs have been installed in the inspection gallery at the base of embankment dams or at the bottom of concrete dams for the purpose of safety control against earthquakes. Most dams in Japan, except for small earth dams, are constructed directly on the excavated bedrock of riverbeds and abutments. The lower part of a massive dam is, roughly considered to behave in the same way as its bedrock and rock abutment during earthquakes. However, the earthquake response of a dam is affected by the dynamic interaction of the dam-foundation-reservoir system. The earthquake waves observed at the dam base or at the dam bottom are interacted especially with its foundation. In other words, the earthquake waves at the dam base are the combination of the incident waves through the foundation and the radiation waves through the dam body. They are, therefore, different from the waves at the free-field, i.e. outcrop. In order to make practical use of the observations at the dam base of the many dams where seismometers have already been installed, it is necessary to evaluate the quantitative difference of the earthquake wave at the dam base with that at the free-field.

The effects of the dynamic interaction between a dam and its foundation are evaluated by wave energy dissipation through the dam to the foundation or by radiation damping. Analytical approaches of radiation damping of embankment dams have been performed (Chopra & Perumalswami 1969, Ohmachi 1980, Yanagisawa 1982, Hirata 1989, Tohei & Ohmachi 1990). In these evaluations, analytical procedures were mainly used and few comparative evaluations with actual dam observations were conducted.

In this paper, we evaluate the effects of frequency contents of input waves and the impedance ratio on

1) Head, Fill Dam Division, Public Works Research Institute, Ministry of Construction, Tsukuba, Japan
2) Senior Research Engineer, ditto

the dynamic interaction between an embankment dam and its foundation. The little effect of a reservoir on an embankment is not considered. The evaluations are performed using both FEM numerical analysis and the earthquake observations at an existing dam. Moreover, we propose a simplified analytical procedure that estimates the incident seismic wave on the basement layer without the dynamic interaction effects from the observations at the base of an embankment dam.

2. DYNAMIC INTERACTION AT BASE OF AN EMBANKMENT DAM

(1) Analytical Method and Cases

We analyzed the two-dimensional FE model of the Miho Dam in Japan, a 95.0 m-high rockfill dam with a central core, shown in Figure 1. The physical and dynamic properties of the dam were determined from in-situ tests and laboratory tests using the fill materials of this dam. We used the complex dynamic response analysis program DINAS, which employs equivalent linear dynamic soil modeling.

We performed analyses on the five cases shown in Table 1. Where, ρ_D is the density of the dam body of 2.3 t/m^3 , ρ_F is the density of the foundation of 2.575 t/m^3 , Vs_D is the S-wave velocity for the dam body of 600m/s , Vs_F is the S-wave velocity for the foundation. In Cases 1A and 1B, the effect of the frequency contents of the input wave on the dynamic interaction was evaluated. In Case 1A, the acceleration wave which has a maximum value of 138.2gal, is shown in Figure 2, and was observed at the downstream toe of the Miho Dam during the event of March 6, 1996 (JMA magnitude of 5.8) was used as input. In Case 1B, the same wave as in Case 1A, with the time axis stretched by a factor of two (that is, with twice calculation period) was used as input. The predominant frequency of the input wave of Case 1B was consistent with the natural frequency of the dam body. In Cases 1B, 2-4, the effects of the impedance ratio between the dam body and its foundation were evaluated by changing the shear stiffness of the foundation.

Table 1 Analytical cases

Case Name	S-wave Velocity for Foundation V_{SF}(m/s)	Impedance Ratio α	Calculation Period Δt(s)	Items Investigated
CASE 1A	1950	0.29	0.01	Frequency contents of input waves
CASE 1B	1950	0.29	0.02	
CASE 2	1380	0.41	0.02	Impedance ratio $\alpha = \frac{\rho_D \cdot V_{SD}}{\rho_F \cdot V_{SF}}$
CASE 3	975	0.57	0.02	
CASE 4	690	0.81	0.02	

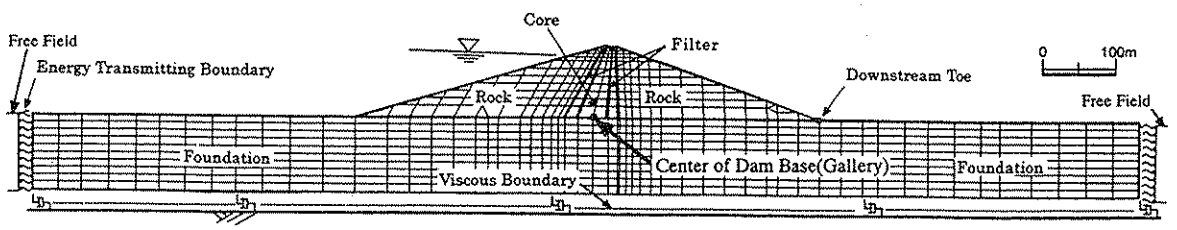

Fig.1 Finite element model of the Miho Dam

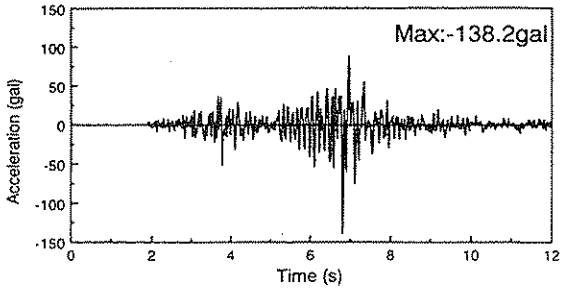

Fig.2(a) Input acceleration-time history for Case 1A

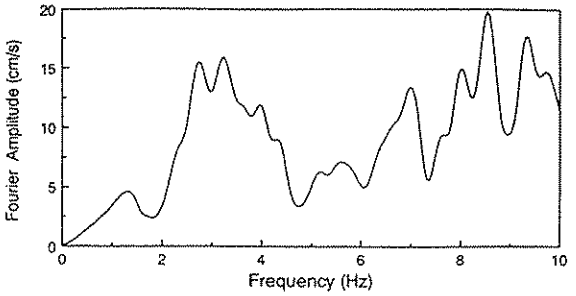

Fig2(b) Fourier amplitude spectrum of input acceleration for Case 1A

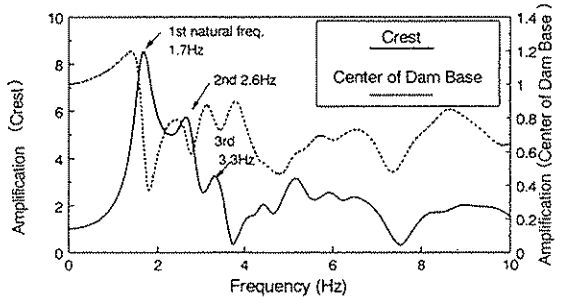

Fig.3 Amplification spectra for Case 1A

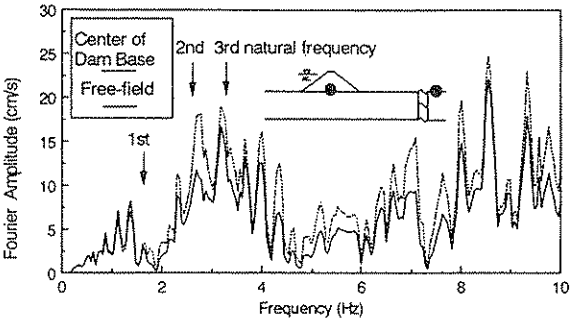

Fig.4 Fourier amplitude spectra of acceleration at dam base and at free-field(Case 1A)

(2) Results of the Analysis

a) Effects of frequency contents of input waves

The amplification spectra of the response waves at the crest and at the center of the dam base against the input wave for Case 1A are shown in Figure 3. The amplification spectrum for the dam base dips at a slightly higher frequency than the natural frequency that is indicated as the predominant frequency of the amplification spectrum at the crest. The amplification spectrum for the dam base in Figure 3 shows that the seismic wave at the dam base reduces the seismic power at the frequency range of the natural frequencies of the dam considerably.

Figure 4 shows the Fourier amplitude spectra of the acceleration at the center of the dam base and at the free-field for Case 1A. The amplitude spectrum for the dam base is smaller than that for the free-field for the second and third natural frequencies of the dam (around 3 Hz). This is because the spectrum of the input wave has large amplitudes around the second and third natural frequencies of the dam. The Fourier

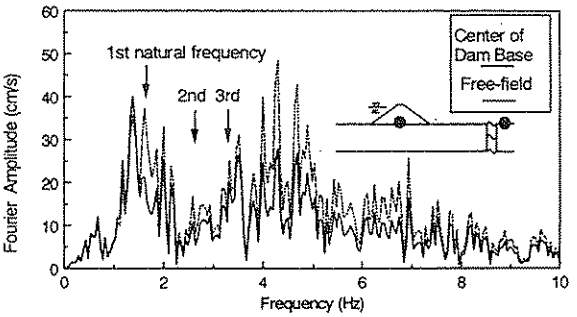

Fig.5 Fourier amplitude spectra of acceleration at dam base and at free-field(Case 1B)

amplitude spectra for Case 1B are shown in Figure 5. The amplitude spectrum for the dam base is considerably smaller than that for the free-field around the first natural frequency of 1.7Hz. When an incident wave that has large energy power around the natural frequency of a dam is input, dynamic interaction between the dam and its foundation makes the spectral amplitude of the response acceleration at the dam base decrease around this frequency.

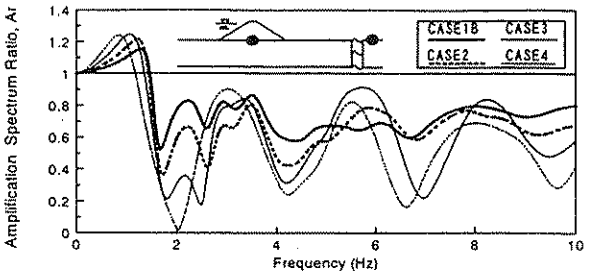

Fig.6 Amplification spectrum ratio for dam base

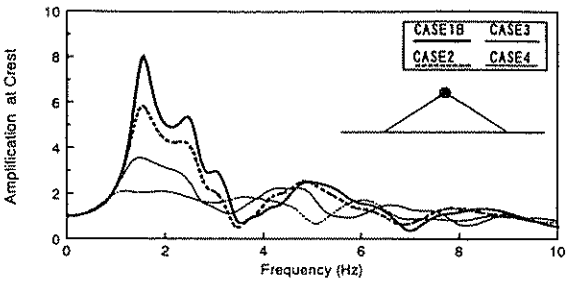

Fig.7 Amplification spectrum for crest

b) Effects of impedance ratio

The amplification spectrum ratio Ar was calculated by dividing the amplification spectrum for the dam base by the one for the free-field. The amplification spectrum ratio Ar shows the difference between the seismic response at the dam base and that at the free-field. Figure 6 shows the amplification spectrum ratios for the central part of the dam base for Cases 1B, 2 to 4. Figure 7 shows the amplification spectrum for the crest. Figure 8 shows the relationship between the frequency where the amplification spectrum ratio for the dam base sinks in Figure 6 and the predominant frequency of the amplification spectrum for the crest in Figure 7. Figure 8 shows that each sinking frequency for the dam base is slightly higher than the corresponding predominant frequency for the crest. Figure 6 shows that the larger the impedance ratio, the larger the dip in the amplification spectrum ratio. In other words, the larger the impedance ratio, the larger the effect of dynamic interaction. Figure 7 shows that as the impedance ratio decreases, so the response magnification of the dam increases. This indicates that the smaller the impedance ratio, the larger the non-linearity of the dam body and the lower its natural frequency. It is, therefore, suggested that the sinking frequency for each amplification spectrum ratio shown in Figure 6 becomes higher as the impedance ratio increases.

Figure 9 shows the distribution of maximum acceleration, which is normalized by dividing by the maximum acceleration at a free-field, along the dam base and on the downstream ground surface for each of the analytical cases. The maximum accelerations are smallest at the center of the dam base and recover as you move toward the downstream toe. The maximum accelerations at the downstream toe are only about ten percent less than the maximum accelerations at the free-field. The larger the impedance ratio, the more the drop of the maximum accelerations at the dam base becomes and the larger the dynamic interaction between the dam and the foundation becomes.

The residual of the amplification spectrum ratio was integrated from 0.5f1 to 2.5f1, where f1 is the first natural frequency. The mean residual e shown in equation (1) represents the ratio of the energy loss at the dam base due to the dynamic interaction.

$$e = \frac{1}{2f_1}\int_{0.5f_1}^{2.5f_1}(1 - Ar(f))df \qquad (1)$$

Figure 10 shows the distribution of the mean residual e along the dam base (footprint) and on the downstream ground surface for each of the analytical cases. The mean residual e is large around the center of the dam base and becomes smaller as you move toward the downstream toe. Furthermore, the larger the impedance ratio, the larger the mean residual, i.e. the larger the energy loss due to dynamic interaction. The values of the mean residual e are only about 0.1 around the downstream toe for all the cases.

Figures 9 and 10 indicate that the effect of dynamic interaction on earthquake response is low around the downstream toe, regardless of the impedance ratio. There is negligible effect of dynamic interaction due to the dam on the seismic response at the point about half a dam's width away from the downstream toe.

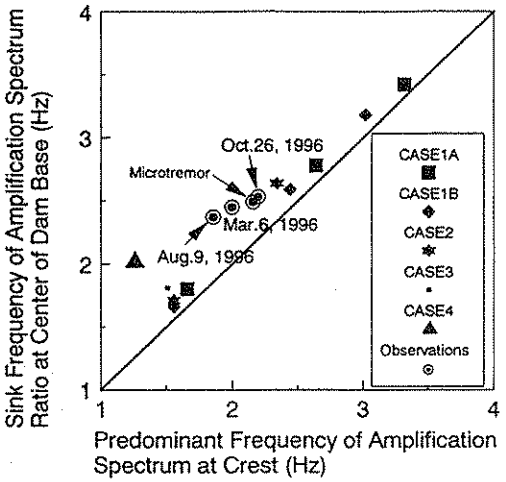

Fig.8 Comparison between sinking frequency of tansfer function ratio for dam base and predominant frequency of transfer function for crest

(3) Verification of Analytical Results Using Observations

The characteristics of the earthquake motions at the dam base obtained from the analytical procedures in part 2.(2) above were verified using the earthquake observations during three events shown in Table 2 and the data of microtremor measurements at the Miho Dam. We calculated the ratio of the Fourier amplitude spectrum of the waves observed at the crest to that at the outcrop. We also calculated the ratio of the Fourier amplitude spectrum of the waves observed at the center of the dam base to that at the outcrop. The relationships between the sinking frequency of the Fourier amplitude spectrum ratio for the center of the dam base and the predominant

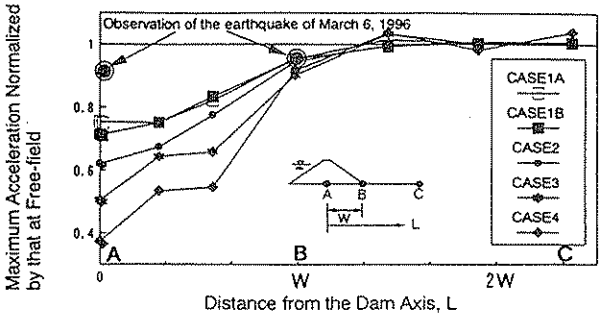

Fig.9 Distribution of maximum acceleration at dam base and downstream ground surface

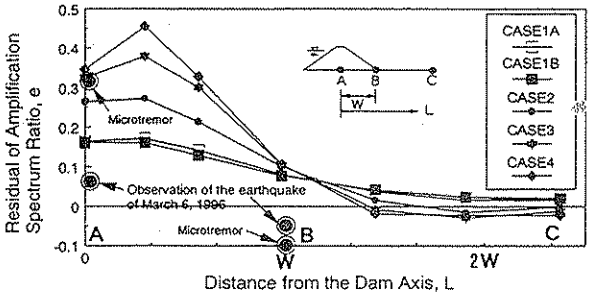

Fig.10 Distribution of mean residual of amplification spectrum ratio for dam base and downstream ground surface

frequency for the crest obtained from the observations and the microtremor data have been added to Figure 8. The points appear slightly above the 45-degree line that represents the case where the sinking frequency for the dam base is equal to the predominant frequency for the crest. In other words, the sinking frequency for the dam base is slightly higher than the corresponding predominant frequency for the crest, which agrees well with the analytical results in part 2.(2) above.

Table 2 Earthquake records at the Miho Dam

Date	Maximum Acceleration (gal)			Epicentral Distance	JMA Magnitude
	Crest	Gallary	Downstream Toe	(km)	
March 6,1996	243.9	84.4	138.2	13	5.8
August 9, 1996	62.3	13.8	21.8	17	4.7
October 26, 1996	15.9	3.4	5.4	11	4.0

The normalized maximum acceleration and the mean residual of the amplification spectrum ratio from the earthquake observations during the event of March 6, 1996 and the microtremor data measured at the center of the dam base and the downstream toe have been added to Figures 9 and 10 respectively. The waves observed at the outcrop were used as the reference wave records. The maximum acceleration at the center of the dam base is smaller than that at the downstream toe. The mean residual e at the center of the dam base is larger than that at the downstream toe. These trends agree with those seen in the analytical results.

3. ESTIMATION OF SEISMIC WAVE INCIDENT ON BASEMENT LAYER

(1) Estimation Procedure

As stated in the previous section, earthquake waves observed at the dam base are interacted with the dam body. Hence, we propose a simplified procedure for estimating the wave incident on the basement layer from observations at the base of an embankment dam analytically. Ohmachi & Kataoka (1995) estimated the incident seismic waves from the observations at the base of a concrete dam using the procedure that involved dividing the frequency characteristics of the observations at the dam base by the transfer function. However, an earth structure such as an embankment dam has the high earthquake-induced non-linearity of the soil and rockfill materials. This is the major difference between an embankment dam and a concrete dam with regard to the estimation of the incident wave for earth structure. For this reason, we performed dynamic equivalent linear pre-analysis on the model of an embankment dam with a rigid foundation. A rigid foundation model is analyzed because the wave observed at the dam base must be input. This dynamic pre-analysis gives the shear modulus of the dam reached in the inelastic region during shaking. Furthermore, a comparison between the analytical response results and other observations at the dam enables the accuracy of the dam model to be verified.

The estimation procedure is illustrated in Figure 11 and described as follows:

STEP 1. The dynamic pre-analysis of the embankment dam model with a rigid foundation is performed using the equivalent linear soil modeling method. The distribution of the shear modulus of the dam in the final iterative calculation step is obtained.
STEP 2. The transfer function for the dam base is calculated using the above shear modulus of the dam.
STEP 3. The Fourier spectrum, which involves the characteristics of both amplitude and phase, of the wave incident on the basement layer is obtained by dividing the Fourier spectrum of the wave observed at the dam base by the above transfer function.
STEP 4. The Fourier inverse transform of the Fourier spectrum calculated above gives the seismic wave incident on the basement layer.

An observed wave consists of the coupled response of horizontal and vertical vibrations. In this simplified procedure, however, we consider only the horizontal transfer function for the horizontal input motion and only the vertical transfer function for the vertical input motion.

(2) Dam Analyzed and its Model

We applied this procedure to the earthquake observations at the Minoogawa Dam during the Kobe Earthquake of 1995. The Minoogawa Dam, a 47.0 m-high rockfill dam, was located about ten kilometers northeast of the earthquake fault. The seismometers installed in the inspection gallery at the base of the dam and at the dam crest recorded acceleration waves during the excitation. Their maximum horizontal accelerations perpendicular to the dam axis were 135 gal in the gallery and 242 gal at the crest. The dam foundation is hard bedrock that has an elastic wave velocity of about 4 km/s. The impedance ratio between the dam and the foundation is about 0.3.

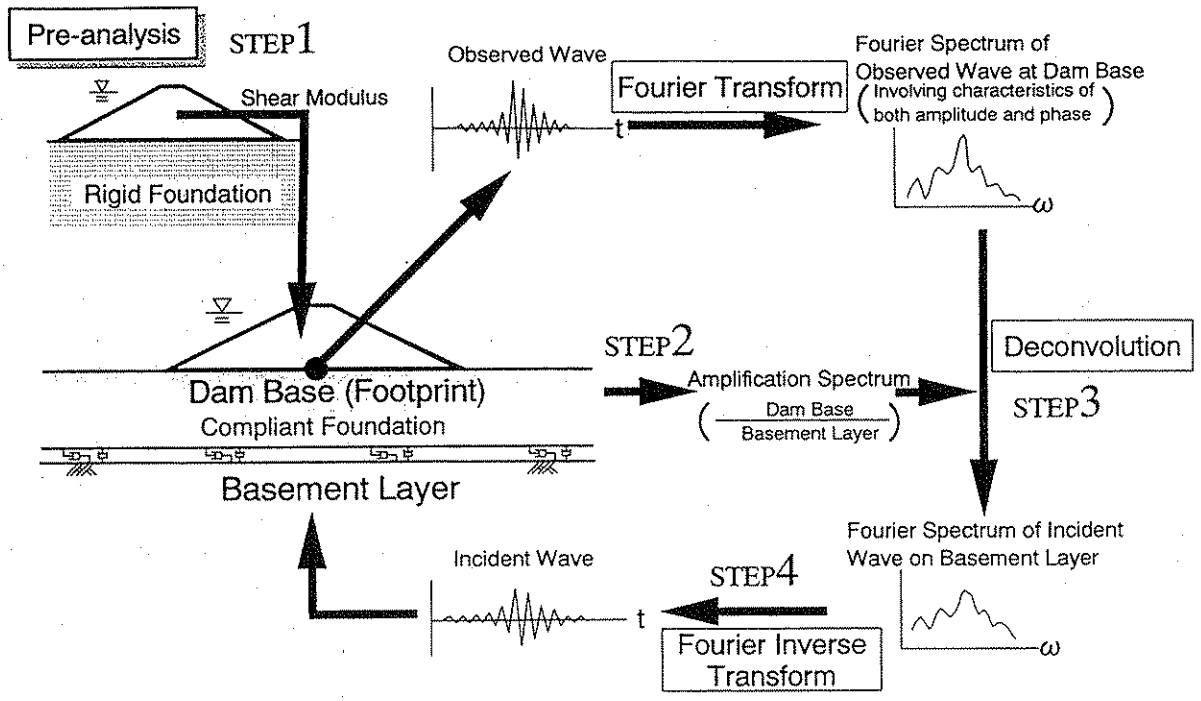

Fig.11 Illustration of the procedure to estimate incident waves

We prepared the 2-D FE model of the cross section of the Minoogawa Dam as shown in Figure 12. The properties of the dam materials were determined from the results of execution control tests in the time of the construction and the laboratory tests using the fill materials of this dam. We verified the accuracy of the vibration characteristics of the model by comparing the natural frequency of the model with that from earthquake observations and microtremor measurements (Iwashita & Yoshida 1997). In the pre-analysis of the rigid foundation model, the effects of energy dissipation by dynamic interaction were assumed to be represented by the equivalent radiation damping ratio that was added to the hysteresis damping ratio of the dam materials.

(3) Calculation of an Incident Wave

First, we analyzed the rigid foundation model and obtained the shear modulus of the dam during excitation. Figure 13 shows comparisons of the observed response acceleration at the crest with that obtained through the dynamic pre-analysis. Looking at the acceleration-time history, during the first half of the principal motion (t = 4 - 6 sec) the analytical results agree well with the observations, but during the second half (over 6 sec) the analytical results are smaller than the observed values. With regard to the Fourier amplitude spectrum, the analytical results in the low frequency range less than 2 Hz agree well with the observations, but the analytical results are

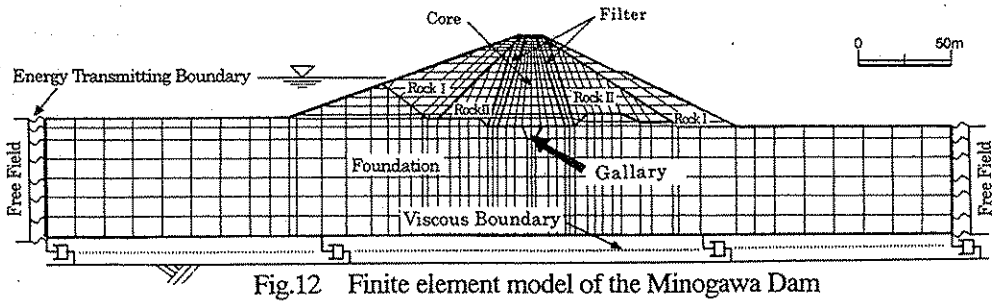

Fig.12 Finite element model of the Minogawa Dam

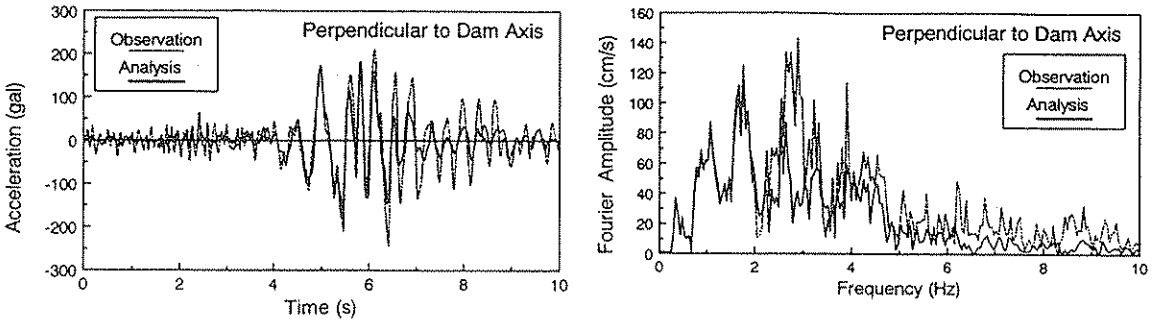

Fig.13 Comparison between observed acceleration at crest with analytical results (pre-analysis of the Minogawa Dam model with a rigid foundation)

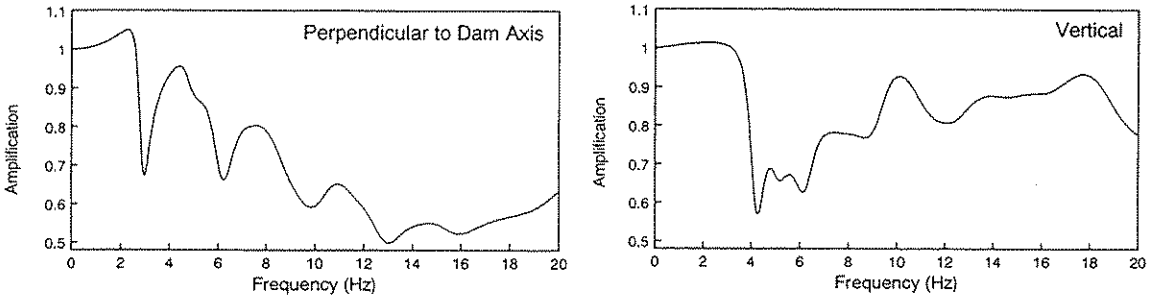

Fig.14 Amplification spectra for the center of the dam base of the Minogawa Dam model

smaller than the observed values around the natural frequency during shaking of 3 Hz. In spite of the rigid foundation model analysis, the analytical results give relatively good agreement with the observations. This confirms that the model describes the non-linearity of the dam during the earthquake quite well.

Secondly, the transfer functions for the dam base were calculated using the shear modulus of the dam, which is the output from the above pre-analysis on the rigid foundation model. The amplification spectra shown in Figure 14 have significant sinking at 3 Hz for the direction perpendicular to the dam axis and at about 4Hz for the vertical direction.

Finally, we estimated the wave incident on the basement layer of the Minoogawa Dam site using steps 3 and 4 of the above-mentioned procedure, with the earthquake observations in the inspection gallery built on the dam base and its transfer functions.

Figure 15 shows that the estimated incident wave time history and Fourier amplitude spectrum. The wave observed at the inspection gallery is also shown in the figures for the shake of comparison. The horizontal maximum accelerations of the incident wave and the wave observed in the gallery are 137 gal and 135 gal respectively; the vertical maximum accelerations are 89 gal and 80 gal respectively. The amplitude spectrum of the incident wave is larger than that for the wave observed at the gallery at the natural frequencies (the range around 3 Hz for the horizontal direction and 4 to 5 Hz for the vertical direction) because of the dynamic interaction effects described in section 2.

(4) Verification of the Estimated Incident Wave

We performed dynamic analysis on the Minoogawa Dam model with a compliance foundation. The incident wave estimated in the previous section was input under the basement boundary of the

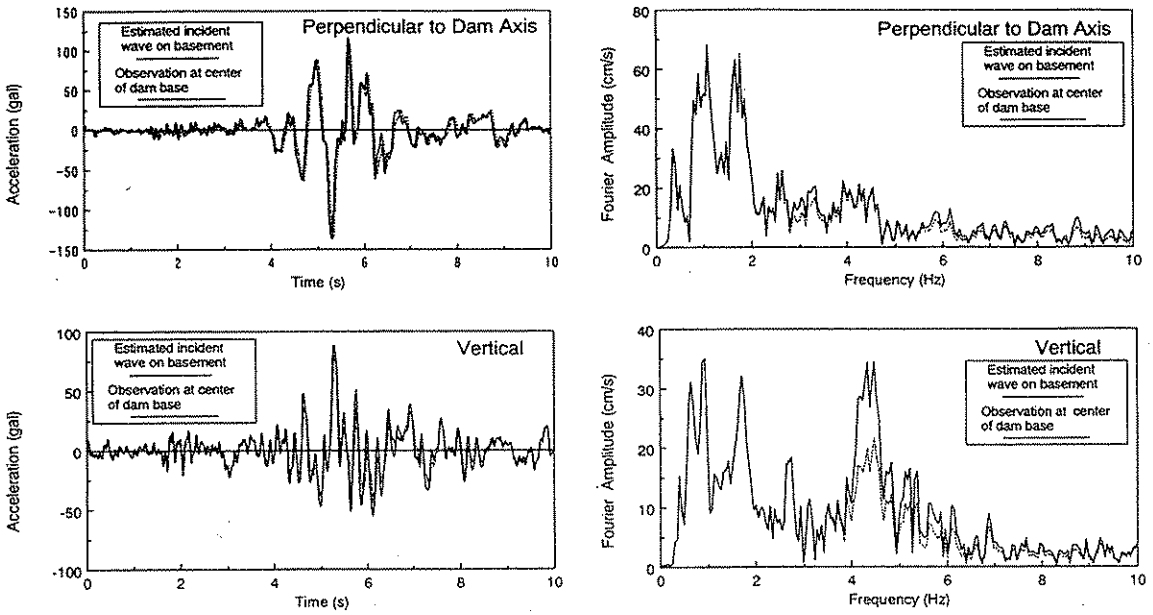

Fig.15 Estimated incident acceleration on basement layer and observed acceleration at dam base

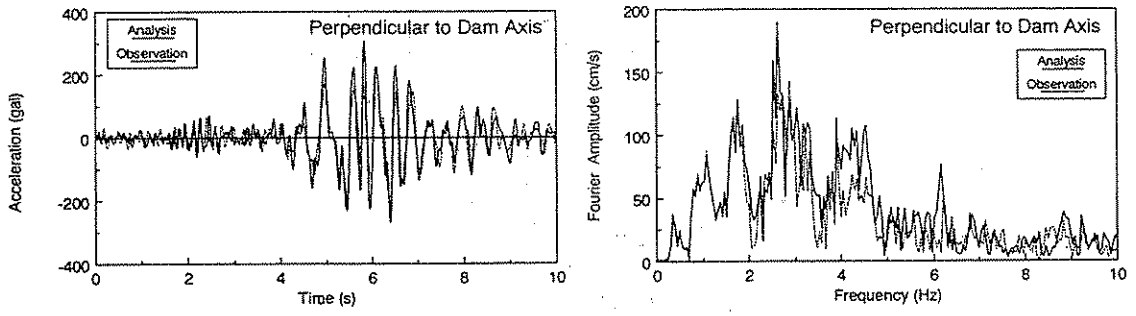

Fig.16 Comparison of observed acceleration at crest with analytical results (analysis on the Minogawa Dam model with a compliant foundation ,on which the estimated incident wave was input)

compliance foundation model. Figure 16 shows the comparisons of the acceleration-time histories and Fourier amplitude spectra of the analytical response horizontal acceleration at the crest with those of the observed acceleration at the crest. The results of the analysis agree with the observations for both the time history and the Fourier spectrum, Of particular note is the good agreement of the time histories even for the second half of the principal motion and of the Fourier amplitudes at around 3 Hz. In the above range, the results from the simulation of the rigid foundation model analysis did not agree with the observations, as shown in Figure13.

4. CONCLUSIONS

(1) Due to the dynamic interaction between an embankment dam and its foundation, the Fourier amplitude of the seismic waves at the dam base at the natural frequency is smaller than that at the free-field. It was demonstrated from FEM analysis and observations at an existing dam that the sinking frequency is slightly higher than the corresponding predominant frequencies for the response wave at the crest.

(2) The larger the Fourier amplitude of the incident seismic wave for the natural frequency of the

dam and the larger the impedance ratio of the dam and its foundation, the larger the dynamic interaction effects become.

(3) Dynamic interaction effects such as reductions in maximum acceleration and wave energy are the largest at the center of the dam base and decrease as you move towards the downstream toe. These interaction effects are fairly small by time you reach the toe. The effects at a point about half a dam's width from the downstream toe are about the same as those at a free-field.

(4) A simplified procedure for estimating the incident wave from the observations at the dam base was proposed. This procedure was demonstrated by estimating the waves incident on the basement layer at the Minoogawa Dam site during the Kobe Earthquake.

REFERENCES

Chopra, A.K. & P.R. Perumalswami (1969): Dam-foundation interaction during earthquakes, *Proc. 4th World Conference on Earthquake Engineering*, pp.37-52.

Hirata, K. (1989): Estimation of radiation damping in dynamic analysis of fill dams, *Report of Central Research Institute of Electric Power Industry*. U88061, CRIEPI.

Iwashita, T. & H. Yoshida (1997): Earthquake response analysis and seismic stability of a rockfill dam –Behavior of the Minoogawa Dam during the Kobe Earthquake–, *Engineering for Dams*. No.126, pp.27-35, Japan Dam Engineering Center.

Ohmachi, T. (1980): A fundamental study on dynamic interactions with a rockfill dam and the foundation deposit, *Tsuchi-to-Kiso*, No.1191, pp.31-36, Japanese Society odf Soil Mechanics and Foundation Engineering.

Ohmachi, T. & S. Kataoka (1995): Evaluation of dynamic interaction effects of 2-D dam-foundation-reservoir systems, *Proc. of the Japan Society of Civil Engineers*, No.519: pp.199-209, Japan Society of Civil Engineers.

Tohei, M. & T. Ohmachi (1990): Model analysis procedure using a FE-BE method in time domain and its application to a dam-foundation system, *Proc. of the Japan Society of Civil Engineers*, 416, pp.429-438, Japan Society of Civil Engineers.

Yanagisawa, E. (1982): Effect of ground condition on vibrational characteristics of earth structure, *Proc. of the Japan Society of Civil Engineers*, No.317, pp.101-110, Japan Society of Civil Engineers.